JGR Oceans

RESEARCH ARTICLE
10.1029/2022JC018931

Drivers, Dynamics, and Persistence of the 2017/2018 Tasman Sea Marine Heatwave

Jules B. Kajtar[1,2], Scott D. Bachman[3], Neil J. Holbrook[1,2], and Gabriela S. Pilo[1,4]

[1]Institute for Marine and Antarctic Studies, University of Tasmania, Hobart, TAS, Australia, [2]Australian Research Council Centre of Excellence for Climate Extremes, University of Tasmania, Hobart, TAS, Australia, [3]Climate and Global Dynamics Laboratory, National Center for Atmospheric Research, Boulder, CO, USA, [4]CSIRO, Oceans & Atmosphere, Hobart, TAS, Australia

Abstract During the austral summer of 2017/2018, the Tasman Sea experienced an intense marine heatwave over an extensive area. It persisted for approximately 3 months and caused substantial ecological impacts. The marine heatwave was understood to have been driven primarily by increased net downward heat flux associated with a high pressure system. However, it has been unclear why the marine heatwave persisted. Using an ultra-high-resolution (~1 km) regional ocean model simulation, the drivers, dynamics, and persistence of the 2017/2018 marine heatwave are explored in detail. It is found that a burst of warm water advection helped to initiate the event, but a shallower than usual mixed layer, coupled with near continuous net downward air-sea heat flux, caused the marine heatwave to persist. Submesoscale dynamics were found to be relatively unimportant to the marine heatwave's persistence.

Plain Language Summary Marine heatwaves are occurrences when the ocean temperature is much warmer than usual for an extended period. A large-scale marine heatwave, lasting around 3 months, occurred in the Tasman Sea between Australia and New Zealand during the austral summer of 2017/2018, causing severe impacts on the local marine ecology. The marine heatwave is known to have been driven by atmospheric heating, but it is unclear why it lasted as long as it did. Using an ultra-high-resolution ocean model simulation, a clearer picture has emerged of how ocean dynamics helped to initiate the marine heatwave, while heating by the atmosphere and a shallower than normal mixed layer caused it to persist.

Key Points:

- An ultra-high-resolution simulation explored the drivers and ocean dynamics in maintaining the record 2017/2018 Tasman Sea marine heatwave
- A warm water burst helped to initiate it, but a shallower than usual mixed layer and ongoing atmospheric heating caused it to persist
- Submesoscale dynamics were found to be relatively unimportant

Correspondence to:
J. B. Kajtar,
jules.kajtar@utas.edu.au

Citation:
Kajtar, J. B., Bachman, S. D., Holbrook, N. J., & Pilo, G. S. (2022). Drivers, dynamics, and persistence of the 2017/2018 Tasman Sea marine heatwave. *Journal of Geophysical Research: Oceans*, *127*, e2022JC018931. https://doi.org/10.1029/2022JC018931

Received 1 JUL 2022
Accepted 12 JUL 2022

Author Contributions:
Conceptualization: Jules B. Kajtar, Scott D. Bachman, Neil J. Holbrook, Gabriela S. Pilo
Formal analysis: Jules B. Kajtar, Scott D. Bachman
Investigation: Jules B. Kajtar, Scott D. Bachman, Neil J. Holbrook, Gabriela S. Pilo
Methodology: Jules B. Kajtar, Scott D. Bachman, Neil J. Holbrook, Gabriela S. Pilo
Resources: Neil J. Holbrook
Software: Scott D. Bachman
Supervision: Neil J. Holbrook
Visualization: Jules B. Kajtar
Writing – original draft: Jules B. Kajtar, Scott D. Bachman, Neil J. Holbrook, Gabriela S. Pilo

1. Introduction

The Tasman Sea, between the southeast of Australia and New Zealand (Figure 1), has experienced much higher warming rates than the global average over the last several decades (Holbrook & Bindoff, 1997; Oliver, Lago, et al., 2018; Ridgway, 2007). Such rising mean ocean temperatures have led to an increase in the frequency, duration, and intensity of marine heatwaves (Oliver, Donat, et al., 2018 Oliver, Lago, et al., 2018), which are prolonged periods of unusually warm sea temperatures (Hobday et al., 2016). Marine heatwaves can have devastating impacts on the marine environment (Cavole et al., 2016; Garrabou et al., 2009; Manta et al., 2018; Mills et al., 2013; Pearce & Feng, 2013; Smale et al., 2019; Wernberg et al., 2013), and those that have occurred in the Tasman Sea are no exception (Oliver et al., 2017; Perkins-Kirkpatrick et al., 2019; Salinger et al., 2019).

Two extreme marine heatwaves occurred in the Tasman Sea in the austral summers of 2015/2016 and 2017/2018. The two events were the most extreme in terms of temperature anomalies and duration in the observed satellite record (since the early 1980s), but also likely in the instrumental record dating back to the late 19th century (Oliver et al., 2017; Perkins-Kirkpatrick et al., 2019). Following the marine heatwave definition of Hobday et al. (2016), and based on daily satellite sea surface temperature (SST) observations, the 2015/2016 event was the longest event on record (251 days; Oliver et al., 2017), and the 2017/2018 event was the next longest (221 days; Perkins-Kirkpatrick et al., 2019). However, the two events were very different in their characteristics, dynamics, and drivers. A detailed study of the 2015/2016 marine heatwave found that the water column warmed to a depth of at least 200 m (Oliver et al., 2017). It was primarily driven by an enhanced southward extension of the East Australian Current (EAC), which transported oceanic heat into the region (Oliver et al., 2017). The 2017/2018 marine heatwave was much shallower, with the warm temperature anomalies confined to ~30–40 m depth (Perkins-Kirkpatrick et al., 2019), as observed in ARGO float measurements (Salinger et al., 2019), but it occurred

Writing – review & editing: Jules B. Kajtar, Scott D. Bachman, Neil J. Holbrook, Gabriela S. Pilo

over a much broader area, extending across the entire longitudinal span of the Tasman Sea (Perkins-Kirkpatrick et al., 2019).

The 2017/2018 marine heatwave has been linked to regional atmospheric forcing. During November 2017, the mean sea level pressure was persistently high over the Tasman Sea (Perkins-Kirkpatrick et al., 2019; Salinger et al., 2019). The marine heatwave was centered on the equatorward flank of the high pressure system, which is typical of atmospherically driven marine heatwaves in the midlatitudes, due to the associated patterns of winds and Ekman flow (Sen Gupta et al., 2020). Although the high pressure system began to weaken and shift eastward past New Zealand from December 2017 (Bureau of Meteorology & NIWA, 2018; Salinger et al., 2019), the anomalously warm SST in the Tasman Sea persisted into February 2018.

Two key details about the 2017/2018 Tasman Sea marine heatwave are not yet well understood: why was it so intense, and why did it persist for so long? It is possible that small scale dynamics in the surface mixed layer, namely submesoscale processes, contributed to both its intensity and persistence. The oceanic submesoscale flow field occupies the 0.1–10 km horizontal spatial scales (Thomas et al., 2008), and submesoscale eddies are mainly generated in the mixed layer by instabilities, frontogenesis, and wind stress (McWilliams, 2016; Wang et al., 2018). It has been found that submesoscale eddy activity is strongest during winter and fall in the midlatitudes, when the mixed layer is deepest due to atmospheric forcing (Dong et al., 2020; Qiu et al., 2017; Sasaki et al., 2014; Wang et al., 2018). Hence, energy conversion scales with mixed layer depth (MLD). This relationship is important because vertical velocities associated with submesoscale dynamics tend to be stronger than for mesoscale features (Fox-Kemper et al., 2008; McWilliams, 2016; Thomas et al., 2008), as verified in high-resolution simulations (Bachman et al., 2017; Couvelard et al., 2015; Rosso et al., 2014). Submesoscale eddies are small and fast, but also powerful, facilitating rapid vertical redistribution of nutrients and tracers, as observed in phytoplankton distributions (Lévy et al., 2018). If the mixed layer was particularly shallow during the 2017/2018 marine heatwave, as would be expected during a period of net ocean heating from the atmosphere, then diminished submesoscale eddies might prevent the downward vertical transport of heat, thus reinforcing the heatwave through positive feedback. This is just one hypothesis for the intensity and persistence of the 2017/2018 event. Another possibility is that there was an additional component of heating due to ocean advection that coupled with persistent air-sea heat flux anomalies over a long duration. Such hypotheses are yet to be tested.

In this study, we investigate the roles of various drivers of the 2017/2018 Tasman Sea marine heatwave in an ultra-high-resolution (0.01°) regional ocean model simulation, in which submesoscale eddies are permitted. Marine heatwaves are generally better represented in models with higher resolution (Pilo et al., 2019), and models with insufficient resolution tend to simulate marine heatwaves that are too weak and longer in duration (Frölicher et al., 2018). With an ultra-high-resolution simulation, we hypothesize that a clearer picture will emerge of why the marine heatwave was so intense, and why it persisted so long. A more complete dynamical history of the event will help to understand the dynamics and evolution of similar atmospherically driven marine heatwaves elsewhere.

2. Data and Methods

2.1. Observational Data

SST is analyzed in two observational products. The first is the daily Optimum Interpolation Sea Surface Temperature (OISST) version 2.1, provided by the National Oceanic and Atmospheric Administration (NOAA; Huang et al., 2021). These data were analyzed over the period from 1982 to 2020. The second is the three-dimensional weekly multi observation (MOB) global ocean product (MULTIOBS_GLO_PHY_TSUV_3D_MYNRT_015_012; Greiner et al., 2020; Guinehut et al., 2012; Mulet et al., 2012) provided by the Copernicus Marine Environment Monitoring Service (CMEMS). SST is taken as the top level of the 3D temperature field from the reprocessed data, and it was analyzed over the period 2014–2019. NOAA OISST and CMEMS MOB are both provided on the same 0.25° spatial grid. In computing a seasonal climatology (i.e., where anomalies are required), the mean temperatures are computed over an 11-day window centered on each calendar day, sampling each year within the baseline period. The climatology is then smoothed by applying a 31-day moving mean. SST anomalies in CMEMS MOB are shown relative to the NOAA OISST 1983–2012 seasonal climatology. Where required, the weekly CMEMS MOB data are linearly interpolated to a daily temporal resolution.

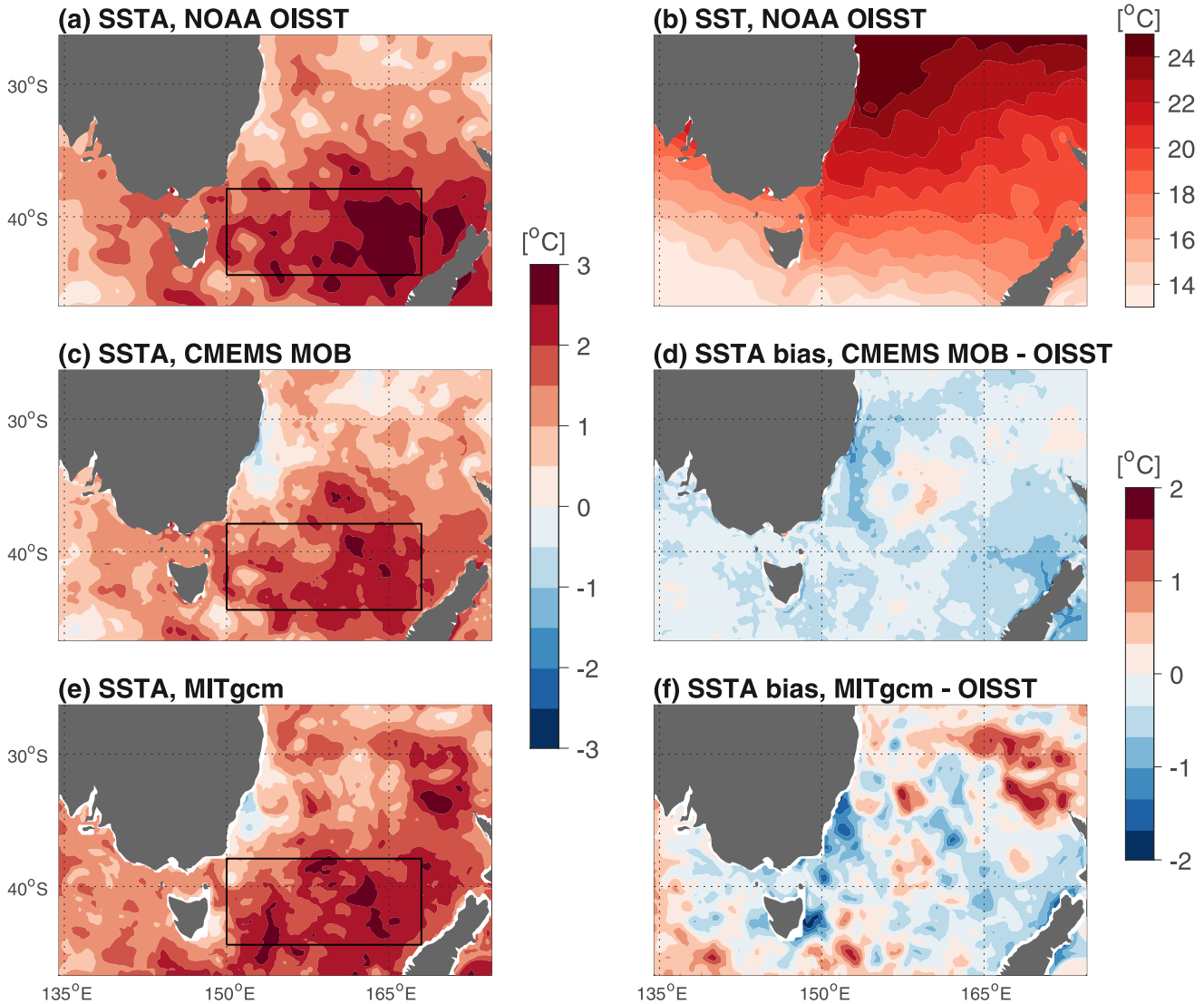

Figure 1. Mean sea surface temperature (SST) during November 2017 to January 2018. (a) SST anomalies (SSTA) relative to the 1983–2012 seasonal climatology in NOAA OISST observations. (b) Absolute SST in NOAA OISST. (c) SSTA in CMEMS multi observations (MOB) relative to 1983–2012 seasonal climatology in NOAA OISST. (d) Difference in SSTA between CMEMS MOB and NOAA OISST. (e) SSTA in the MITgcm simulation relative to 1983–2012 seasonal climatology in NOAA OISST, but where the area average of the mean MITgcm SST field is first bias corrected to match NOAA OISST over November 2017 to January 2018. (f) Difference in SSTA between MITgcm and NOAA OISST. Due to the applied bias correction, the area average of this field is zero. In the left panels, the Tasman Sea region analyzed in this study (150°–168°E, 44°–38°S) is denoted by a black box. Where differences between products were required, the data were first bilinearly interpolated to the NOAA OISST grid.

MLD is also analyzed in CMEMS MOB, but rather than using the provided 2D MLD variable, it is calculated from the 3D temperature and salinity fields. A density-based MLD definition is used, with a variable threshold on the potential density (σ) profile (de Boyer Montégut et al., 2004), such that the MLD is the depth at which $\sigma = \sigma_{10} + \Delta\sigma$. Here σ_{10} is the density at 10 m depth, and:

$$\Delta\sigma = \sigma\left(T_{10} - 0.2\,^{\circ}\mathrm{C},\ S_{10}, P_0\right) - \sigma\left(T_{10},\ S_{10}, P_0\right), \tag{1}$$

where T_{10} and S_{10} are the temperature and salinity at 10 m, respectively, and $P_0 = 0$ db is the surface pressure. In other words, the MLD is where the density increases from the 10 m density due to a prescribed temperature decrease of 0.2°C from the 10 m temperature, whilst maintaining constant salinity (value at 10 m). The Gibbs-SeaWater Oceanographic Toolbox (McDougall & Barker, 2011) is used to compute the density fields

from the given temperature and salinity fields. As with SST in CMEMS MOB, the MLD was analyzed over the period 2014–2019.

2.2. MITgcm Simulation

A regional ocean model simulation of the 2017/2018 Tasman Sea marine heatwave was conducted with the Massachusetts Institute of Technology general circulation model (MITgcm; Marshall et al., 1997). The single 0.01° resolution simulation was conducted over the period 1 January 2016 to 30 April 2018 (28 months), for the region 134.5°–174.5°E, 46°–26°S (Figure 1). The horizontal resolution of ∼1 km is sufficient to permit the simulation of submesoscale eddies. The vertical grid consisted of 100 layers of varying thickness, with 5 m layers for the top 100 m, and then gradually increasing to 100 m layers beyond 1,000 m depth. The maximum depth was 5,844 m. Surface variables were output at hourly frequency, but all variables analyzed herein are daily means. The initial state and boundary conditions were from the CMEMS Operational Mercator global ocean analysis and forecast system, which is provided at 1/12° resolution (GLOBAL_ANALYSIS_FORECAST_PHY_001_024). Atmospheric conditions throughout the simulation were from the operational archive of the European Center for Medium-Range Weather Forecasts (ECMWF) atmospheric analysis. Other details of the simulation follow those given by Bachman et al. (2017). Due to the computational expense, only a single simulation was conducted. The use of initial and boundary conditions from a coarser product may result in some biases or drift, and such details will be examined.

SST is taken as the top layer of the 3D temperature field, which represents the temperature of the uppermost 5 m of the ocean. Hence this is not identical to the way satellite observational SST is measured, but any differences due to this effect are expected to be minor. Comparisons between model and observational SST are made in Section 3.1. The MLD is calculated in the same way as for the observational data (Section 2.1): using a density-based MLD definition with a variable threshold on the density profile.

2.3. Temperature Tendency Budget

In order to accurately analyze the temperature tendency budget, the full set of budget terms were output from the model during November to March in 2016/2017 and 2017/2018. The complete budget includes advection, surface heat flux, diffusion, a surface mass correction to account for the linear free surface, and the K-Profile Parameterization for vertical mixing. It was verified that the sum of these terms matched the temperature tendency for a given volume to at least nine decimal places. The analysis here focuses on the advection terms (including a decomposition to meridional, zonal, and vertical components), and the surface heat flux. Hence the temperature tendency (time rate of change of temperature T), $\frac{\partial T}{\partial t}$, volume-averaged within a given upper ocean mixed layer of depth H and horizontal area A is:

$$\frac{\partial |T|}{\partial t} = -|\mathrm{v} \cdot \nabla T| + \frac{1}{A}\int^{A} \frac{Q}{\rho C_p H} dA + \text{residual} \tag{2}$$

where $|\cdot| = \frac{1}{HA}\int^{A}\int_{-H}^{0} \cdot dz dA$, $\mathbf{v}$ is the 3D fluid velocity vector, Q is the total air-sea heat flux (including contributions from sensible and latent heat flux, as well as shortwave and longwave radiation), and ρ and C_p are the density and specific heat capacity of seawater, respectively. The residual includes diffusive and parameterized mixing terms, and it is typically small relative to the air-sea heat flux and advection terms.

2.4. Mesoscale and Submesoscale Decomposition

To determine the contribution to the temperature tendency budget of different spatial scales, some variables have been decomposed. A variable, here for example, vertical velocity w, can be decomposed into its temporal mean, $\overline{w}$, mesoscale, $\langle w \rangle$, and submesoscale, w', components, such that:

$$w = \overline{w} + \langle w \rangle + w'. \tag{3}$$

The temporal mean is computed over the entire 28 months of the simulation. The mesoscale term is computed by applying a horizontal 20 grid-point (i.e., ∼20 km) lowpass filter in the form of a 2D convolution of $\left(w - \overline{w}\right)$

with a constant square window (e.g., Rosso et al., 2014). The submesoscale components (e.g., w') are therefore represented by spatial variations smaller than the 20 km horizontal length scale. Submesoscale eddies evolve on time scales in the order of a few days (e.g., Thomas et al., 2008), and therefore analysis at daily temporal resolution is sufficient. The decomposition is applied to w and T such that the mean, mesoscale, and submesoscale components of the vertical advection term in the temperature tendency can be analyzed. Only vertical advection is decomposed in this way since that is the term of primary interest.

3. Results

3.1. Characteristics of the Marine Heatwave

Unusually warm sea surface temperature anomalies (SSTA) extended across the entirety of the Tasman Sea between southeast Australia and New Zealand during the 2017/2018 marine heatwave. The 3-month average SST from 1 November 2017 to 31 January 2018 was at least 1°C above average over most of the region, and large parts of the eastern Tasman Sea experienced 2°C above average (Figures 1a and 1c).

The MITgcm simulation (Figures 1e and 1f) exhibits a cold bias in SST relative to NOAA OISST, which is partly related to the fact that the top 5 m layer in MITgcm is compared to the skin temperature from satellite observations. From November 2017 to January 2018, and area averaged over the region shown in Figure 1, the cold bias in MITgcm is −0.81°C. The CMEMS MOB is also cooler than NOAA OISST by −0.35°C (Figure 1d). After bias correcting the area average mean temperature in MITgcm to match NOAA OISST, the large-scale features in the spatial pattern of SSTA are in reasonable agreement with observations (Figures 1e and 1f). Note that the SSTA field in CMEMS MOB is not corrected (Figures 1c and 1d). The warm bias in MITgcm east of 165°E and north of 35°S is most likely due to a stronger than observed Tasman Front (a.k.a. eastern extension of the EAC; Oke et al., 2019). Though not a direct comparison, the mean eastward flow through moorings at ∼168°E between ∼30° and 32°S was 6.4 Sv over July 2003 to August 2004, with a standard deviation of 4.9 Sv (Sutton & Bowen, 2014). The simulated eastward flow is 17.4 Sv during 2017, with a standard deviation of 5.5 Sv.

The timeseries of the central Tasman Sea area average SST (150°–168°E, 44°–38°S; region indicated in Figures 1a, 1c and 1e) shows that the temperature increased sharply, by almost 4°C in a matter of days, in early November 2017 (Figure 2a). The region entered a marine heatwave state (following the Hobday et al., 2016 definition) on 14 November 2017, in which it remained until 19 February 2018. The sharp rise in temperature took the marine heatwave to Category 3 (or "severe", following the Hobday et al., 2018 intensity classification), in which it spent a total of 27 days throughout its 98-day duration. The discrepancy in the duration here as compared with Perkins-Kirkpatrick et al. (2019) is due to differences in the selected domains and the baseline climatology periods. The area average SST peaked at ∼21°C in late January 2018, which is the record maximum for the region in the observational period. Although the marine heatwave terminated in February 2018, the temperature hovered near the 90th percentile level until April 2018, before dropping back toward the climatological mean (Figure 2a). The SSTA timeseries shows that the temperature was >2°C above average for most of December 2017 and January 2018 (Figure 2b), and above the range of temperatures from all other years over the period 1982–2020. The cold bias in the MITgcm simulation is most apparent in the warmer months (Figure 2a), but variations in temperature largely align with observations. After the mean SSTA from October 2017 to March 2018 in MITgcm is matched with that in NOAA OISST, the simulated SSTA closely follows the observed during the marine heatwave period (Figure 2b).

The range in MLD (also area averaged over the region indicated in Figures 1a, 1c and 1e) is typically between ∼30 and 170 m in CMEMS MOB (Figure 2c). The simulated MLD generally agrees well with CMEMS MOB, apart from some higher frequency variability, which is not captured in the weekly observational data, and the much deeper simulated mixed layer in the cooler months. The MLD shoaled to ∼20 m from mid-November 2017 and remained so for several months (Figure 2d). It was at its shallowest in almost every week during the 2017/2018 marine heatwave, in the albeit short (2014–2019) observational record. The simulated MLD is also shallower during most of 2017/2018 as compared to 2016/2017 (Figure 2d).

The evolution of temperature and salinity depth profiles are shown in Figure 3. The seasonal cycle is apparent in temperature down to ∼200 m, and in the MLD (Figure 3a), but less so for salinity (Figure 3). Stronger temperature anomalies are mostly confined to the MLD (Figure 3c), but exceptions (e.g., during June–July 2017) might have occurred due to periods of deeper vertical advection. In particular, the warm anomalies associated

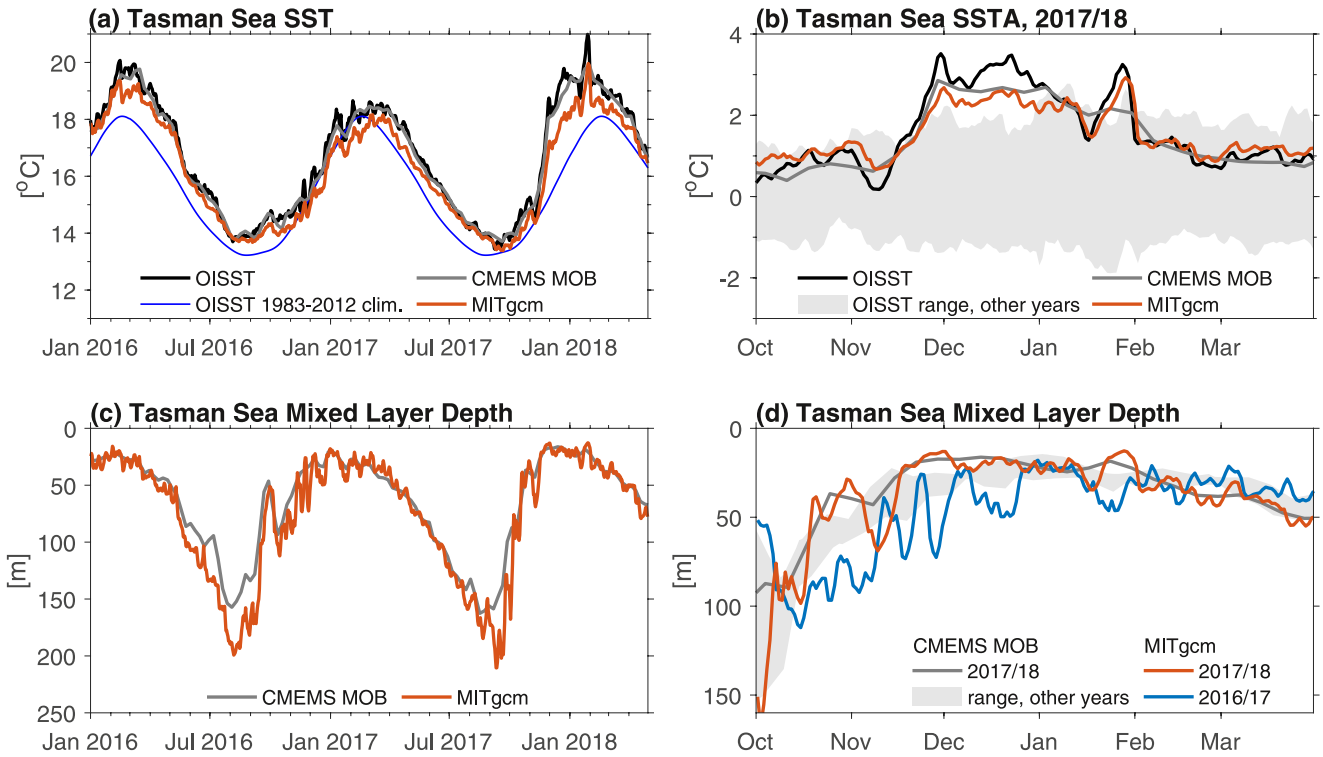

Figure 2. Area average sea surface temperature (SST) and mixed layer depth in the Tasman Sea (150°–168°E, 44°–38°S). (a) SST over a 28-month period leading up to the marine heatwave, in observational products and the MITgcm simulation. The blue curve denotes the 1983–2012 smoothed seasonal climatology in NOAA OISST. (b) SST anomalies (SSTA) relative to the 1983–2012 seasonal climatology in NOAA OISST. The MITgcm SSTA is bias corrected such that the mean SSTA during October 2017 to March 2018 matches that from NOAA OISST. Gray shading denotes the NOAA OISST range in every year other than 2017/2018, during October 1982 to March 2020. (c) Mixed layer depth over a 28-month period in observations and MITgcm. (d) Mixed layer depth during October to March, shown for 2016/2017 and 2017/2018 in MITgcm, and 2017/2018 in CMEMS multi observations (MOB). Gray shading denotes the CMEMS MOB range in every year other than 2017/2018, during October 2014 to March 2020.

with 2017/2018 marine heatwave are almost completely confined to the mixed layer. In the area average sense, the warm temperature anomalies are within a maximum depth of <40 m. There is a positive salinity anomaly associated with the marine heatwave, but its magnitude is not particularly striking, at least in comparison to other salinity anomalies during that time (Figure 3d). One caveat for this analysis is that the anomalies are relative to the short 2014–2019 climatology, and warm temperature anomalies might be stronger given a longer baseline (due to the long-term warming trend). As seen in SST, the mostly cool bias in the MITgcm simulation extends to depths of 1,500 m (Figure 3e). The salinity is under-represented by the model in the upper layers, but over-represented near ∼1,100 m depth (Figure 3f). There also appears to be some drift in the simulated temperature and salinity which, as noted earlier, may be due to the coarser initial and boundary conditions provided.

3.2. Temperature Tendency Budget

A temperature tendency budget analysis was conducted over the central Tasman Sea region (as shown in Figures 1a, 1c and 1e) to a depth of 55 m (Figure 4). This depth was selected because it is below the observed mean MLD of ∼50 m in early November and ∼20 m in early January (Figure 2d). The temperature tendency budget indicates that the 2017/2018 Tasman Sea marine heatwave was primarily driven by net downward air-sea heat flux (Figure 4). Throughout most of the duration of the marine heatwave (November 2017 to January 2018), the atmospheric heating is positive, and it is responsible for the majority of the total temperature tendency (Figure 4d). The SSTA closely follow the atmospheric heating tendency throughout this period, as well as the MLD variations (Figure 4b). Air-sea heat flux tends to be positive throughout the marine heatwave, despite the fact that the high pressure system over the Tasman Sea in November 2017 had shifted eastward of New Zealand by December (Bureau of Meteorology & NIWA, 2018; Salinger et al., 2019).

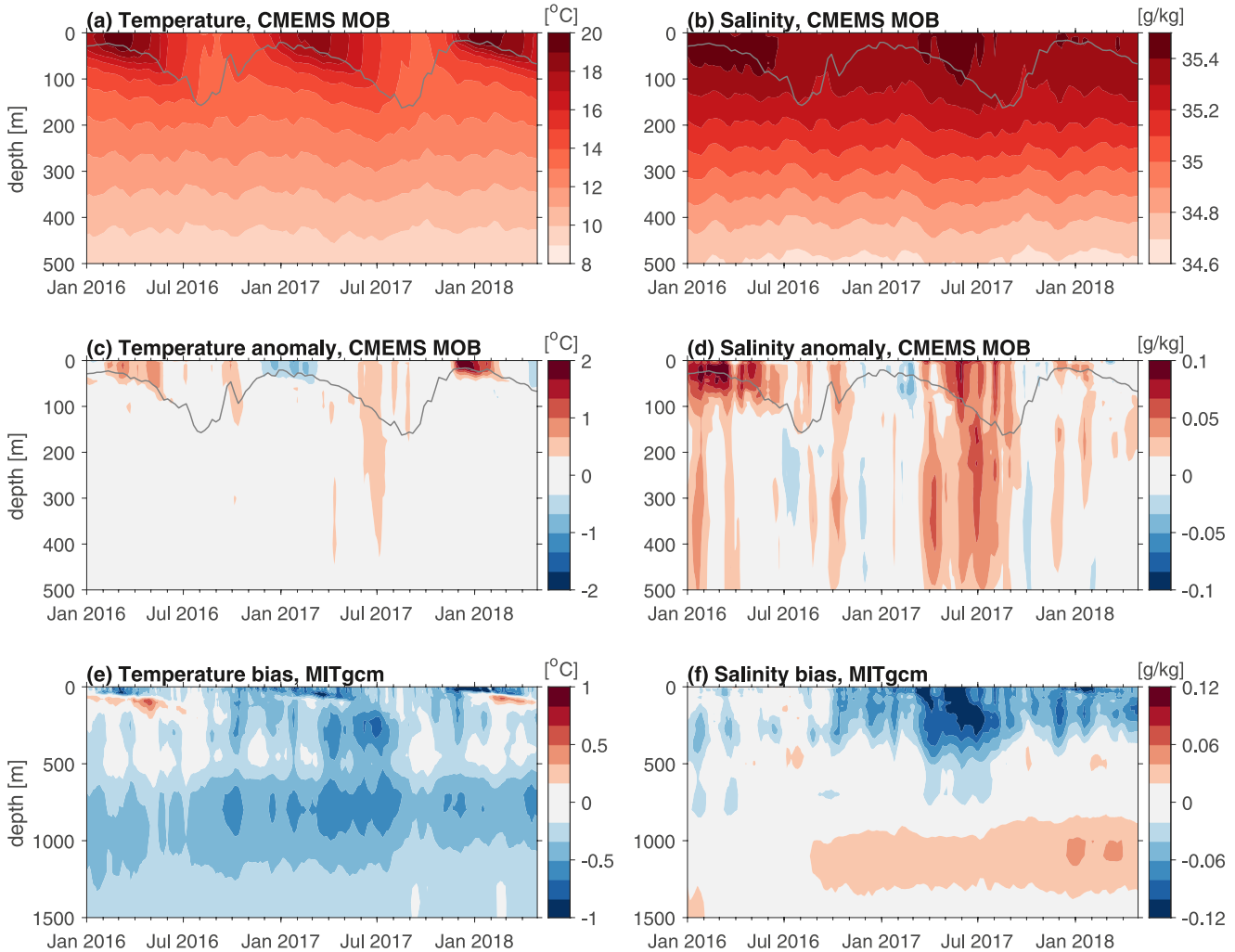

Figure 3. Depth profiles of temperature and salinity, area averaged in the Tasman Sea (150°–168°E, 44°–38°S). (a) Temperature over a 28-month period leading up to the marine heatwave in CMEMS multi observations (MOB). The gray curve, which is also in (b–d), is the CMEMS MOB mixed layer depth. (b) Salinity in CMEMS MOB. (c) Temperature anomaly in CMEMS MOB, relative to the 2014–2019 climatology. (d) Salinity anomaly in CMEMS MOB, relative to the 2014–2019 climatology. (e) Temperature bias in the MITgcm simulation (i.e., MITgcm minus CMEMS MOB). (f) Salinity bias in the MITgcm simulation.

The air-sea heat flux tends to be the main contribution to the total temperature tendency throughout both 2016/2017 and 2017/2018 (Figures 4c and 4d), which is partly due to the selected volume spanning only a relatively shallow layer (55 m). But not all prolonged periods of atmospheric heating triggered a marine heatwave. There is a month-long period commencing mid-December 2016 (Figure 4c), for instance, during which SSTA were not substantially above average (Figure 4a). An interesting feature in the temperature tendency budget during the 2017/2018 marine heatwave is that from early-November 2017, there is a month-long period during which there is nearly continual advective heating (Figure 4d). This is one of the more pronounced periods of advective heating in the two periods shown (Figures 4c and 4d), and it is more clearly seen in the 10-day moving average (Figures 4e and 4f). It is compelling that this period of advective heating occurs during the onset of the marine heatwave, even though the integrated advective heating contributes only approximately one quarter of the total temperature tendency during that time. The residual in the temperature tendency, comprised of diffusive and parameterized mixing terms (Section 2.3) is generally small, and close to negligible during November 2017, but it does become comparable to the magnitude of the advection term after February 2018 (Figure 4d).

A decomposition of the temperature tendency due to advection (Figures 4e and 4f) shows that a strong meridional component in November 2017 was not completely offset by the zonal and vertical components, resulting in the net advective heating at that time (Figure 4f). Thus, the 2017/2018 marine heatwave appears to have

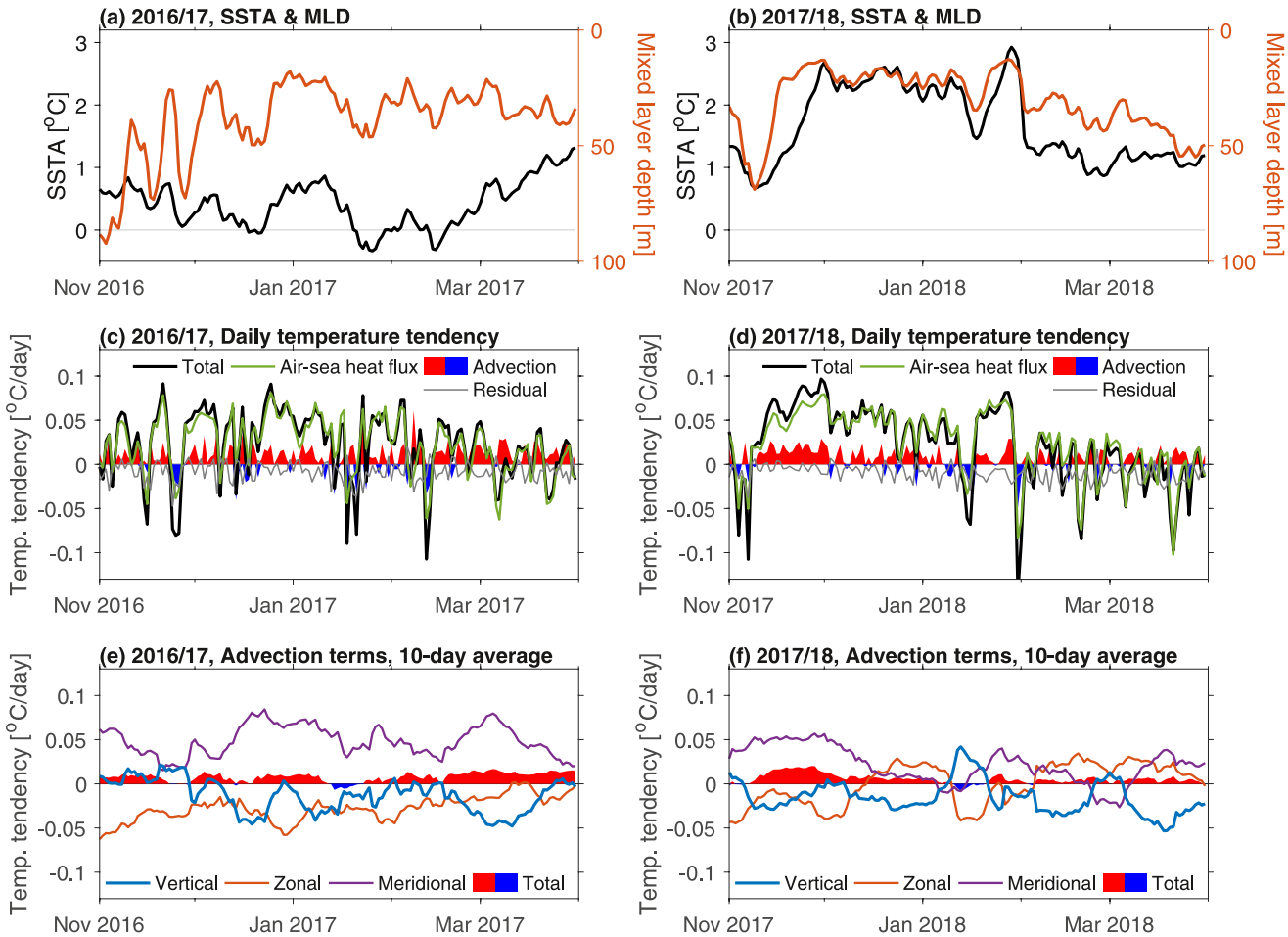

Figure 4. MITgcm temperature tendency budget in the Tasman Sea (150°–168°E, 44°–38°S) over the top 55 m. (a, b) MITgcm sea surface temperature anomalies (SSTA) and mixed layer depth (MLD) in 2016/2017 and 2017/2018. SSTA is relative to the 1983–2012 seasonal climatology in NOAA OISST, and it is bias corrected to match the mean SSTA in NOAA OISST during October to March over each year separately. (c, d) Tasman Sea temperature tendency budget to a depth of 55 m. The total includes all terms in the full temperature tendency budget, which is the sum of the air-sea heat flux, advection, and the residual. The residual includes diffusive and parameterized mixing terms. Daily temperature tendency is shown. (e, f) Tasman Sea temperature tendency contributions from vertical, zonal, and meridional advection terms. Total denotes the sum of the vertical, zonal, and meridional terms, and it is equivalent to the advection terms shown in (c, d). However, note that 10-day moving means of each term are shown here, as distinct from the daily data shown in (c, d).

been initiated by a period of advective heating, which was coupled with an atmospheric heating-induced rapid shoaling of the MLD by ~50 m over a 2–3 week period (Figure 4b). The shoaling of the MLD is seasonal, but it is more pronounced in November 2017 than in the previous year when it was much more variable and did not shoal to the same level (Figure 4a; see also Figure 2d).

The marine heatwave appears to have been terminated by a strong cooling air-sea signal that occurred over ~2–3 days in late January 2018 (Figures 4b and 4d), likely linked to a short but sharp low pressure system traversing the region. An earlier air-sea cooling signal, in mid-January, did not terminate the marine heatwave, but did cause a slight drop in the SSTA (Figures 4b and 4d). The marine heatwave persisted through that period since the air-sea heat flux rebounded strongly for a further 2 weeks. In the following section, we test the role of submesoscale dynamics in causing the marine heatwave to persist.

3.3. Mesoscale and Submesoscale Vertical Heat Advection

To investigate the extent to which the submesoscale dynamics prolonged the marine heatwave (by inhibiting downward temperature transport), the vertical velocity and temperature at 55 m depth were decomposed into their mean, mesoscale, and submesoscale components (Section 2.4). The timeseries of the various vertical temperature

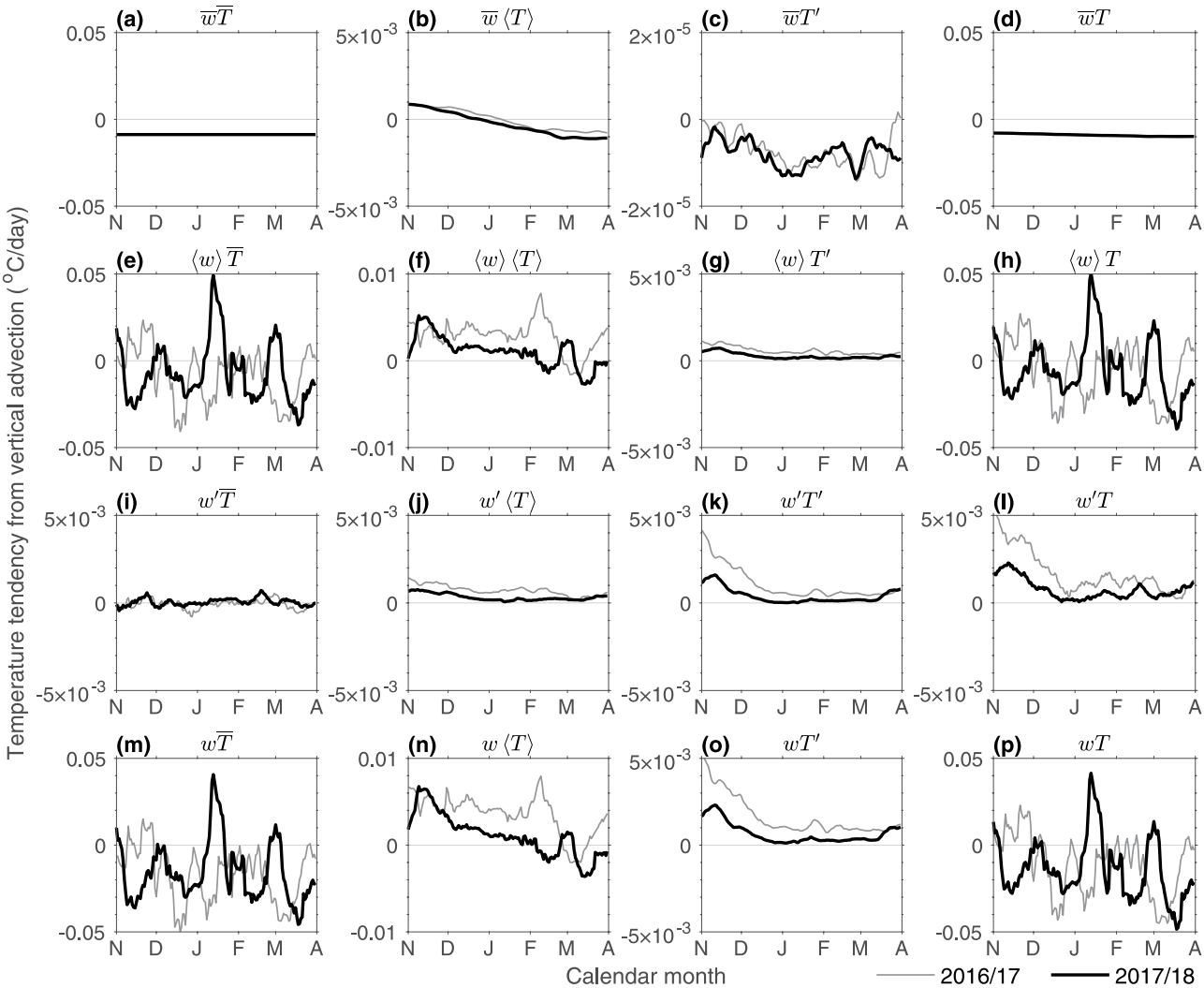

Figure 5. MITgcm temperature tendency due to vertical advection in the Tasman Sea (150°–168°E, 44°–38°S) at 55 m depth. All products of vertical velocity (w) and temperature (T) are shown for completeness, including long term mean $\left(\overline{w},\overline{T}\right)$, mesoscale ($\langle w\rangle,\langle T\rangle$), and submesoscale components (w',T'), during November to March in 2016/2017 and 2017/2018. The panels in the final row and column show the sum of the terms in the preceding panels in the same column and row. For example, $w\overline{T}$ (panel (m)) is equal to $\overline{w}\overline{T}+\langle w\rangle\overline{T}+w'\overline{T}$ (panels (a, e, and i), respectively). Similarly, the terms in (d) are the sums of the terms in (a–c). The temperature tendency from vertical advection is simply wT divided by the depth of the volume (55 m). Ten-day moving means of each term are shown. Note that the vertical axis range is not the same in each panel.

tendency terms are averaged over the central Tasman Sea region and shown for November to March in both 2016/2017 and 2017/2018 (Figure 5). In the long-term mean, negative $\overline{w}\overline{T}$ denotes cooling, or net downward heat advection through the 55 m layer (Figure 5a). In both periods, the terms with submesoscale components, that is, $w'T$ (Figure 5l) and wT' (Figure 5o), but also seen for $w'\langle T\rangle$, $\langle w\rangle T'$, and $w'T'$ (Figures 5g, 5j and 5k), all follow the MLD evolution, in that they approach zero as the mixed layer shoals. The terms are positive in November of both years, indicating the net upward heat advection by the submesoscales, and then diminish toward zero. But the submesoscale terms are all of a weaker magnitude, with less temporal variability, in 2017/2018 as compared to 2016/2017. This is as expected, since, as shown earlier, the mixed layer is shallower during the marine heatwave.

The magnitudes of the submesoscale terms are small relative to the mean (Figure 5a) and net (Figure 5p) terms. For example, the magnitude of $w'T$ (Figure 5l) and wT' (Figure 5o) approaching mid-November 2017, are approximately an order of magnitude smaller than wT (Figure 5p) at the same time. Similarly, the magnitudes of the terms with submesoscale components tend to be smaller than those with mesoscale components (cf. Figure 5e with 5i, Figure 5f with 5j, Figure 5b with 5c, and Figure 5f with 5g). This indicates that the submesoscale

dynamics did not play a substantial role in diminishing the net vertical temperature transport during the marine heatwave. The weakening of the submesoscale dynamics coupled with the shallower than usual mixed layer may have prevented a small amount of vertical heat advection, particularly during early December 2017 (Figure 5p), but atmospheric heating of the upper ocean was the more substantial driver of the marine heatwave over its entire duration. The sensitivity of the vertical heat advection analysis to the choice in area was tested by dividing the box into two, with one box spanning 150°–159°E, 44°–38°S, and the other 159°–168°E, 44°–38°S, and Figure 5 was reproduced for the two new regions (figures not shown). There were only minor differences in those results, with the overall finding remaining unchanged: that the submesoscale terms are small relative to the other terms.

4. Discussion and Conclusions

The 2017/2018 Tasman Sea marine heatwave was broad in areal extent, intense in temperature, and long in duration. The three facets together are somewhat surprising for an atmospherically driven marine heatwave that was relatively shallow, with maximum depth of <40 m in the area average. Using an ultra-high-resolution (0.01°) regional ocean model simulation with prescribed atmospheric conditions, the drivers, dynamics, and evolution of the marine heatwave have been analyzed. It is shown that throughout its duration, the marine heatwave was predominantly driven by net downward air-sea heat flux, which was mostly continuous for approximately 3 months. However, meridional oceanic heat advection during November 2017 helped to initiate the heatwave, which was coupled with a stronger than usual and prolonged seasonal shoaling of the mixed layer.

The Tasman Sea, recognized as a global warming "hot-spot", has received much attention, not only for the marine heatwaves that have occurred there (e.g., Elzahaby et al., 2021; Z. Li et al., 2020; Oliver, Lago, et al., 2017, 2018; Perkins-Kirkpatrick et al., 2019; Salinger et al., 2019), but also for its relationship with the EAC (e.g., J. Li et al., 2021; Ypma et al., 2015). A study of marine heatwaves in four smaller subdomains of the Tasman Sea found that 53% were primarily driven by air-sea heat flux, and 21% by ocean advection, with the remainder due to a combination of the two drivers (Elzahaby et al., 2021). Another study of a single, but larger, domain found that 51% of marine heatwaves were driven by ocean advection (Z. Li et al., 2020). It has also been found that marine heatwaves driven by ocean advection tended to be four times longer on average than those driven by air-sea heat flux (Elzahaby et al., 2021), exemplifying the unusual nature of the 2017/2018 Tasman Sea marine heatwave in the context of its persistence compared with most other air-sea heat flux driven events in the region.

The ultra-high-resolution simulation permitted the examination of the submesoscale dynamics at ∼1–20 km horizontal length scales. It was found that whilst the vertical heat transport was diminished in the submesoscales, it had little effect on the net vertical heat transport. This was somewhat surprising, since it is understood that vertical velocities associated with submesoscale dynamics tend to be stronger than from the mesoscales (Fox-Kemper et al., 2008; McWilliams, 2016; Thomas et al., 2008), and submesoscale vertical mixing is important for ocean ecology (Lévy et al., 2018). It has also recently been argued that submesoscale ocean eddies can inhibit variability in El Niño–Southern Oscillation (Wang et al., 2022), although in that study a length scale of 600 km delineates the cut-off between mesoscale and submesoscale, rather than a suggested cut-off of ∼10 km (Thomas et al., 2008).

In conclusion, we found that submesoscale dynamics did not play a significant role, at least over the large spatial extent, in prolonging the 2017/2018 Tasman Sea marine heatwave. Although it is computationally costly to run the necessary high-resolution simulations, we consider there may be merit in exploring the role of submesoscale dynamics in other examples of atmospherically driven marine heatwaves. Submesoscale hindrance of net downward vertical heat transport might be more clearly seen in examples where the atmospheric heat-flux is on a smaller spatial extent, or for a shorter duration. In the case of the 2017/2018 Tasman Sea marine heatwave, the large, intense, and continued net downward air-sea heat flux may have overwhelmed the efficacy of the submesoscale dynamics. The marine heatwave was unprecedented in its intensity, and found to be virtually impossible to have occurred without anthropogenic forcing (Perkins-Kirkpatrick et al., 2019). This study has shown that coincident ocean heat advection helped to initiate the marine heatwave, and it catalogs its temperature, MLD, salinity, and heat budget evolution. Our findings motivate further exploration of other marine heatwaves that are considered atmospherically driven, since ocean dynamics may also be important to their initiation, intensity, and/or duration.

Data Availability Statement

The NOAA 0.25-degree daily Optimum Interpolation Sea Surface Temperature (OISST), Version 2.1 description and metadata is available at: https://doi.org/10.25921/RE9P-PT57, and annual datafiles are provided courtesy of NOAA/OAR/ESRL PSL at https://psl.noaa.gov/data/gridded/data.noaa.oisst.v2.highres.html. The Copernicus Marine Environment Monitoring Service (CMEMS) weekly multi observation (MOB) global ocean product (MULTIOBS_GLO_PHY_TSUV_3D_MYNRT_015_012) is available at https://resources.marine.copernicus.eu/product-detail/MULTIOBS_GLO_PHY_TSUV_3D_MYNRT_015_012/INFORMATION. The MITgcm model output, for the variables analyzed herein, is publicly available at http://dx.doi.org/10.25914/GGHK-TD61. The Gibbs SeaWater (GSW) oceanographic toolbox is available at https://www.teos-10.org/software.htm.

Acknowledgments
JBK and NJH acknowledge ongoing support from the Australian Research Council Centre of Excellence for Climate Extremes (CLEX; CE170100023). The authors thank Paola Petrelli of the CLEX CMS team for helping to publish the model output online. The National Computational Infrastructure, which is supported by the Australian Government, was utilized for processing and analyzing the data. The authors thank the National Oceanic and Atmospheric Administration (NOAA) for making available their OISST data set, and the European Union Copernicus Marine Service Information for providing their MOB and global ocean products. Some analysis was conducted using the Gibbs SeaWater (GSW) oceanographic toolbox, and the authors thank T.J. McDougall and P.M. Barker for making the code freely available. The authors wish to thank the two anonymous reviewers and the Editor for their careful examination and constructive reviews which helped to substantially improve this manuscript. Open access publishing facilitated by University of Tasmania, as part of the Wiley - University of Tasmania agreement via the Council of Australian University Librarians.

References

Bachman, S. D., Taylor, J. R., Adams, K. A., & Hosegood, P. J. (2017). Mesoscale and submesoscale effects on mixed layer depth in the Southern Ocean. *Journal of Physical Oceanography*, *47*, 2173–2188. https://doi.org/10.1175/JPO-D-17-0034.1

Bureau of Meteorology, & NIWA. (2018). Special Climate Statement - record warmth in the Tasman Sea, New Zealand and Tasmania. Retrieved from https://niwa.co.nz/sites/niwa.co.nz/files/SCS-joint-2017-18-tasman-sea-heatwave-final.pdf

Cavole, L. M., Demko, A. M., Diner, R. E., Giddings, A., Koester, I., Pagniello, C. M. L. S., et al. (2016). Biological impacts of the 2013–2015 warm water anomaly in the northeast Pacific: Winners, losers, and the future. *Oceanography*, *29*, 273–285. https://doi.org/10.5670/oceanog.2016.32

Couvelard, X., Dumas, F., Garnier, V., Ponte, A. L., Talandier, C., & Treguier, A. M. (2015). Mixed layer formation and restratification in presence of mesoscale and submesoscale turbulence. *Ocean Modeling*, *96*, 243–253. https://doi.org/10.1016/j.ocemod.2015.10.004

de Boyer Montégut, C., Madec, G., Fischer, A. S., Lazar, A., & Iudicone, D. (2004). Mixed layer depth over the global ocean: An examination of profile data and a profile-based climatology. *Journal of Geophysical Research: Oceans*, *109*, C12003. https://doi.org/10.1029/2004JC002378

Dong, J., Fox-Kemper, B., Zhang, H., & Dong, C. (2020). The seasonality of submesoscale energy production, content, and cascade. *Geophysical Research Letters*, *47*, e2020GL087388. https://doi.org/10.1029/2020GL087388

Elzahaby, Y., Schaeffer, A., Roughan, M., & Delaux, S. (2021). Oceanic circulation drives the deepest and longest marine heatwaves in the East Australian Current System. *Geophysical Research Letters*, *48*, e2021GL094785. https://doi.org/10.1029/2021GL094785

Fox-Kemper, B., Ferrari, R., & Hallberg, R. (2008). Parameterization of mixed layer eddies. Part I: Theory and diagnosis. *Journal of Physical Oceanography*, *38*, 1145–1165. https://doi.org/10.1175/2007JPO3792.1

Frölicher, T. L., Fischer, E. M., & Gruber, N. (2018). Heatwaves under global warming. *Nature*, *560*, 360–364. https://doi.org/10.1038/s41586-018-0383-9

Garrabou, J., Coma, R., Bensoussan, N., Bally, M., Chevaldonné, P., Cigliano, M., et al. (2009). Mass mortality in Northwestern Mediterranean rocky benthic communities: Effects of the 2003 heat wave. *Global Change Biology*, *15*, 1090–1103. https://doi.org/10.1111/j.1365-2486.2008.01823.x

Greiner, E., Verbrugge, N., Mulet, S., & Guinehut, S. (2020). Multi Observation Global Ocean 3D Temperature Salinity Heights Geostrophic Currents and MLD Product. Quality Information Document. E.U. Copernicus Marine Service Information [Online]. Retrieved 24 November 2021 Documented in https://catalogue.marine.copernicus.eu/documents/QUID/CMEMS-MOB-QUID-015-012.pdf

Guinehut, S., Dhomps, A.-L., Larnicol, G., & Le Traon, P.-Y. (2012). High resolution 3-D temperature and salinity fields derived from in situ and satellite observations. *Ocean Science*, *8*, 845–857. https://doi.org/10.5194/os-8-845-2012

Hobday, A. J., Alexander, L. V., Perkins-Kirkpatrick, S. E., Smale, D. A., Straub, S. C., Oliver, E. C. J., et al. (2016). A hierarchical approach to defining marine heatwaves. *Progress in Oceanography*, *141*, 227–238. https://doi.org/10.1016/j.pocean.2015.12.014

Hobday, A. J., Oliver, E. C. J., Sen Gupta, A., Benthuysen, J. A., Burrows, M. T., Donat, M. G., et al. (2018). Categorizing and naming marine heatwaves. *Oceanography*, *31*, 162–173. https://doi.org/10.5670/oceanog.2018.205

Holbrook, N. J., & Bindoff, N. L. (1997). Interannual and decadal temperature variability in the southwest Pacific Ocean between 1955 and 1988. *Journal of Climate*, *10*, 1035–1049. https://doi.org/10.1175/1520-0442(1997)010<1035:IADTVI>2.0.CO;2

Huang, B., Liu, C., Banzon, V., Freeman, E., Graham, G., Hankins, B., et al. (2021). Improvements of the Daily Optimum Sea Surface Temperature (DOISST) version 2.1. *Journal of Climate*, *34*, 2923–2939. https://doi.org/10.1175/JCLI-D-20-0166.1

Lévy, M., Franks, P. J. S., & Smith, K. S. (2018). The role of submesoscale currents in structuring marine ecosystems. *Nature Communications*, *9*, 4758. https://doi.org/10.1038/s41467-018-07059-3

Li, J., Roughan, M., & Kerry, C. (2021). Variability and drivers of ocean temperature extremes in a warming western boundary current. *Journal of Climate*, *35*, 1097–1111. https://doi.org/10.1175/JCLI-D-21-0622.1

Li, Z., Holbrook, N. J., Zhang, X., Oliver, E. C. J., & Cougnon, E. A. (2020). Remote forcing of Tasman Sea marine heatwaves. *Journal of Climate*, *33*, 5337–5354. https://doi.org/10.1175/JCLI-D-19-0641.1

Manta, G., de Mello, S., Trinchin, R., Badagian, J., & Barreiro, M. (2018). The 2017 record marine heatwave in the southwestern Atlantic Shelf. *Geophysical Research Letters*, *45*, 12449–12456. https://doi.org/10.1029/2018GL081070

Marshall, J., Adcroft, A., Hill, C., Perelman, L., & Heisey, C. (1997). A finite-volume, incompressible Navier Stokes model for studies of the ocean on parallel computers. *Journal of Geophysical Research: Oceans*, *102*, 5753–5766. https://doi.org/10.1029/96JC02775

McDougall, T. J., & Barker, P. M. (2011). Getting started with TEOS-10 and the Gibbs Seawater (GSW) Oceanographic Toolbox. SCOR/IAPSO WG127. Documented in https://www.teos-10.org/pubs/Getting_Started.pdf

McWilliams, J. C. (2016). Submesoscale currents in the ocean. *Proceedings of the Royal Society A: Mathematical, Physical, and Engineering Sciences.*, *472*, 20160117. https://doi.org/10.1098/rspa.2016.0117

Mills, K. E., Pershing, A. J., Brown, C. J., Chen, Y., Chiang, F. S., Holland, D. S., et al. (2013). Fisheries management in a changing climate: Lessons from the 2012 ocean heat wave in the Northwest Atlantic. *Oceanography*, *26*, 191–195. https://doi.org/10.5670/oceanog.2013.27

Mulet, S., Rio, M.-H., Mignot, A., Guinehut, S., & Morrow, R. (2012). A new estimate of the global 3D geostrophic ocean circulation based on satellite data and in situ measurements. *Deep Sea Research Part II: Topical Studies in Oceanography*, *77*(80), 70–81. https://doi.org/10.1016/j.dsr2.2012.04.012

Oke, P. R., Pilo, G. S., Ridgway, K., Kiss, A., & Rykova, T. (2019). A search for the Tasman Front. *Journal of Marine Systems*, *199*, 103217. https://doi.org/10.1016/j.jmarsys.2019.103217

Oliver, E. C. J., Benthuysen, J. A., Bindoff, N. L., Hobday, A. J., Holbrook, N. J., Mundy, C. N., & Perkins-Kirkpatrick, S. E. (2017). The unprecedented 2015/2016 Tasman Sea marine heatwave. *Nature Communications*, *8*, 1038. https://doi.org/10.1038/ncomms16101

Oliver, E. C. J., Donat, M. G., Burrows, M. T., Moore, P. J., Smale, D. A., Alexander, L. V., et al. (2018). Longer and more frequent marine heatwaves over the past century. *Nature Communications*, *9*, 1324. https://doi.org/10.1038/s41467-018-03732-9

Oliver, E. C. J., Lago, V., Hobday, A. J., Holbrook, N. J., Ling, S. D., & Mundy, C. N. (2018). Marine heatwaves off eastern Tasmania: Trends, interannual variability, and predictability. *Progress in Oceanography*, *161*, 116–130. https://doi.org/10.1016/j.pocean.2018.02.007

Pearce, A. F., & Feng, M. (2013). The rise and fall of the "marine heat wave" off Western Australia during the summer of 2010/2011. *Journal of Marine Systems*, *111–112*, 139–156. https://doi.org/10.1016/j.jmarsys.2012.10.009

Perkins-Kirkpatrick, S. E., King, A. D., Cougnon, E. A., Grose, M. R., Oliver, E. C. J., Holbrook, N. J., et al. (2019). The role of natural variability and anthropogenic climate change in the 2017/2018 Tasman Sea marine heatwave. *Bulletin of the American Meteorological Society*, *100*, S105–S110. https://doi.org/10.1175/BAMS-D-18-0116.1

Pilo, G. S., Holbrook, N. J., Kiss, A. E., & Hogg, A. M. (2019). Sensitivity of marine heatwave metrics to ocean model resolution. *Geophysical Research Letters*, *46*, 14604–14612. https://doi.org/10.1029/2019GL084928

Qiu, B., Nakano, T., Chen, S., & Klein, P. (2017). Submesoscale transition from geostrophic flows to internal waves in the northwestern Pacific upper ocean. *Nature Communications*, *8*, 14055. https://doi.org/10.1038/ncomms14055

Ridgway, K. R. (2007). Long-term trend and decadal variability of the southward penetration of the East Australian Current. *Geophysical Research Letters*, *34*, L13613. https://doi.org/10.1029/2007GL030393

Rosso, I., Hogg, A. M., Strutton, P. G., Kiss, A. E., Matear, R. J., Klocker, A., & van Sebille, E. (2014). Vertical transport in the ocean due to submesoscale structures: Impacts in the Kerguelen region. *Ocean Modeling*, *80*, 10–23. https://doi.org/10.1016/j.ocemod.2014.05.001

Salinger, M. J., Renwick, J., Behrens, E., Mullan, A. B., Diamond, H. J., Sirguey, P., et al. (2019). The unprecedented coupled ocean-atmosphere summer heatwave in the New Zealand region 2017/2018: Drivers, mechanisms, and impacts. *Environmental Research Letters*, *14*, 044023. https://doi.org/10.1088/1748-9326/ab012a

Sasaki, H., Klein, P., Qiu, B., & Sasai, Y. (2014). Impact of oceanic-scale interactions on the seasonal modulation of ocean dynamics by the atmosphere. *Nature Communications*, *5*, 5636. https://doi.org/10.1038/ncomms6636

Sen Gupta, A., Thomsen, M., Benthuysen, J. A., Hobday, A. J., Oliver, E. C. J., Alexander, L. V., et al. (2020). Drivers and impacts of the most extreme marine heatwaves events. *Scientific Reports*, *10*, 19359. https://doi.org/10.1038/s41598-020-75445-3

Smale, D. A., Wernberg, T., Oliver, E. C. J., Thomsen, M. S., Harvey, B. P., Straub, S. C., et al. (2019). Heatwaves threaten global biodiversity and the provision of ecosystem services. *Nature Climate Change*, *9*, 306–312. https://doi.org/10.1038/s41558-019-0412-1

Sutton, P. J. H., & Bowen, M. (2014). Flows in the Tasman Front south of Norfolk Island. *Journal of Geophysical Research: Oceans*, *119*, 3041–3053. https://doi.org/10.1002/2013JC009543

Thomas, L. N., Tandon, A., & Mahadevan, A. (2008). Submesoscale processes and dynamics. In *Ocean modeling in an eddying regime*, *Geophysical Monograph Series* (Vol. 177, pp. 17–38). American Geophysical Union. https://doi.org/10.1029/177GM04

Wang, S., Jing, Z., Liu, H., & Wu, L. (2018). Spatial and seasonal variations of submesoscale eddies in the Eastern tropical Pacific Ocean. *Journal of Physical Oceanography*, *48*, 101–116. https://doi.org/10.1175/JPO-D-17-0070.1

Wang, S., Jing, Z., Wu, L., Cai, W., Chang, P., Wang, H., et al. (2022). El Niño/Southern Oscillation inhibited by submesoscale ocean eddies. *Nature Geoscience*, *15*, 112–117. https://doi.org/10.1038/s41561-021-00890-2

Wernberg, T., Smale, D. A., Tuya, F., Thomsen, M. S., Langlois, T. J., de Bettignies, T., et al. (2013). An extreme climatic event alters marine ecosystem structure in a global biodiversity hotspot. *Nature Climate Change*, *3*, 78–82. https://doi.org/10.1038/nclimate1627

Ypma, S. L., van Sebille, E., Kiss, A. E., & Spence, P. (2015). The separation of the East Australian Current: A Lagrangian approach to potential vorticity and upstream control. *Journal of Geophysical Research: Oceans*, *121*, 758–774. https://doi.org/10.1002/2015JC011133